Brittle-ductile analogue models of fold-and-thrust belts developed during progressive arching: the effect of viscous basal layer pinch-outs

Modelos analógicos frágil-dúctiles de cinturones de pliegues y cabalgamientos desarrollados durante un arqueamiento progresivo: el efecto de la desaparición de la capa viscosa basal

Alejandro Jiménez-Bonilla[1], Ana Crespo Blanc[1], Juan Carlos Balanyá Roure[2], Inmaculada Expósito[2] and Manuel Díaz-Azpiroz[2]

[1] Departamento de Geodinámica-Instituto Andaluz Ciencias de la Tierra, Universidad de Granada-CSIC. Universidad de Granada, 18071. Granada, España

[2] Departamento de Sistemas Físicos, Químicos y Naturales, Universidad Pablo de Olavide. Carretera Utrera km. 1, 41013, Sevilla, España

ABSTRACT

Two brittle-ductile analogue models of fold-and-thrust belts developed during progressive arching that include silicone pinch-outs either perpendicular or parallel to the backstop apex motion direction (AMD) have been performed to test their role in fold-and-thrust belt geometry and structural evolution. When the silicone pinch-out is oriented perpendicular to the AMD the deformation front stagnates at the silicone pinch-out and arc-parallel lengthening is accommodated by normal and strike-slip faults. When deformation progresses, the wedge thickens and collapses, developing dismantling units. In contrast, when silicone pinch-outs are parallel to the AMD, different structural styles appear along the fold-and-thrust belt: a foreland verging imbricate system where silicone is absent, and a doubly-verging system where silicone is present, both separated by transfer zones. Additionally, the absence of silicone gives place to fold and thrust belt segments relatively narrower in plan-view and vertically thickened. Both models could be useful to delve into both the deposition of dismantling units and the distribution of along-strike structural differences observed in the Gibraltar Arc fold-and-thrust belt.

Key-words: *detachment level, fold-and-thrust belt, analogue modeling, progressive arc, Gibraltar Arc*

RESUMEN

Se han realizado dos modelos analógicos frágil-dúctiles de pliegues y cabalgamientos desarrollados durante un arqueamiento progresivo que estudian el efecto de la geometría de los límites de la capa dúctil basal, perpendicular o paralela a la dirección de movimiento del ápex (AMD). El objetivo es caracterizar la geometría del cinturón de pliegues y cabalgamientos, así como su evolución estructural. Cuando el límite de silicona es perpendicular al AMD la deformación avanza hasta el límite de la silicona y el estiramiento paralelo al arco es acomodado por fallas normales y de salto en dirección. Después, la cuña se engrosa y colapsa desarrollando unidades de desmantelamiento. Cuando los límites de silicona son paralelos al AMD se observan diferentes estilos estructurales a lo largo del cinturón de pliegues y cabalgamientos: un sistema imbricado vergente al antepaís donde la silicona está ausente y un sistema doble-vergente en presencia de la silicona, ambos separados por zonas de transferencia. Además, la ausencia de silicona da lugar a segmentos de cinturones de pliegues y cabalgamientos estrechos en planta y verticalmente engrosados. Ambos modelos son útiles para investigar el depósito de unidades de desmantelamiento y la distribución de las diferencias estructurales observadas a lo largo del cinturón de pliegues y cabalgamientos del arco de Gibraltar

Palabras clave: *nivel de despegue, cinturón de pliegues y cabalgamientos, modelización analógica, arco progresivo, Arco de Gibraltar*

Introducción

The external fold-and-thrust belts of Mediterranean Arcs, in particular that around the Gibraltar Arc, are characterized by outward radial thrusting, arc-parallel extension and block vertical-axis rotations accommodated by thin-skinned fold and thrusts, conjugate strike-slip faults and normal faults (*e.g.,* Crespo-Blanc *et al.,* 2015). In the northern branch of the Gibraltar Arc, the distribution of these structural elements seems to depend on the geometry and thickness of the weak upper Triassic (Keuper) evaporites that are the main Subbetic fold-and-thrust belt detachment level (Barcos *et al.,* 2015; Jiménez-Bonilla *et al.,* 2016b).

As Jiménez-Bonilla *et al.* (2016b) has shown, analogue models are useful to understand the structural evolution and kinematics of fold-and-thrust belts in progressive arcs. We used a similar experimental approach, with a protruding indenter and sand and silicone as analogue materials.

This paper introduces new variables by varying the orientation of the ductile layer pinch-out. Experimental results will permit us to: (1) characterize the distribution, geometry and kinematics of the resulting struc-

tures, (2) examine the influence of the pinch-out geometry on the across and along-strike structural style variations and (3) compare our models with the structural evolution of the Gibraltar Arc fold-and-thrust belt.

Model Set Up

The experiments were run in the Analogue Modeling Laboratory of the Geodynamics Department – Earth Science Andalusian Institute in Granada. They were performed in a 66 cm long and 100 cm wide sandbox, floored by a drafting film sheet and confined at the experiment borders by sand (Fig. 1). The initial configuration was formed by quartz sand (1.5 or 2 cm thick) underlain by silicone (0 or 0.5 cm thick), which simulate the brittle behavior of sedimentary rocks and the ductile evaporites, respectively. A 3 cm-side reference grid was sieved on top of the parallelepiped to study the deformation and vertical-axis rotations. The backstop that indents in the parallelepiped is flexible and its curvature ratio diminished while its protrusion grade increased, as shown in figures 1 and 2 (see also Jiménez-Bonilla *et al.*, 2016a). The apex indenter velocity was 0.85 cm/hour and the total displacement was ca. 40 cm. The scaling and physical properties of the analogue materials is described

in Crespo-Blanc (2008) and Jiménez-Bonilla *et al.*, (2016).

Depending on the angle between the weak layer pinch-out and the backstop apex motion direction (AMD), two types of experiments have been performed (Fig. 1). The underlying silicone layer pinch-out is orthogonal to the AMD in Model 1, and parallel in Model 2 (Figs. 1 and 2). Where the silicone was absent, it was replaced by a layer of sand, in such a way that the initial parallelepiped had a constant thickness of 2cm.

The deformation sequence was recorded by time lapse overhead photography. In one of the models, the sand was carefully removed at the end of the experiment in order to observe the silicone topography, whereas, some cross-sections were made in the other (in this case a thin layer of white sand was sieved on top of the parallelepiped before cutting).

Results

Both models resulted in curved fold-and-thrust belts with a high strain partitioning. Their deformation sequence can be observed in figure 2. Shortening was accommodated by thrusts and backthrusts whereas arc-parallel lengthening was accommodated by normal faults and conjugate strike-slip faults. The resulting structural trend line draws salients and recesses in plan view (Figs. 3A and 3B). Both normal and strike-slip faults bounded blocks that rotated up to 40° clockwise and anti-clockwise in the left and right arc limbs, respectively (Fig. 2).

In Model 1, the first structures to nucleate were thrusts and backthrusts detached within the viscous basal layer, of which, the main structure is the frontal thrust that nucleated in the front limit of the silicone (Fig. 2A.1). A relatively undeformed block remained in the apex part bounded by a dextral strike-slip fault in the left arc limb (Fault 5) and a diffuse fault zone formed by strike-slip and normal faults in the right arc limb (Faults 7 and 10), and a frontal thrust (Fault 3), which slightly overcomes the silicone pinch out (in dashed line). In the left side of the model, a thrust formed as a result of border effect (thrust 11).

As deformation proceeded, the central block started to shorten by the formation of a break-thrust sheet and subsequent back-thrust and oblique strike-slip faults (Faults 12, 14 and 15, Fig. 2.A2). At the internal

parts of both arc limbs, some transpressive bands nucleated (*e.g.,* Fault 16 of Fig. 2.A2).

Then, no new thrust formed and deformation continued by thickening of the wedge (stages 2A.3 and 2A.4). Besides, some normal faults at high angles to the main thrusts nucleated (Fault 17, Fig. 2.A3).

Sand slumped and silicone extruded at the front of the wedge forming salt sheets, both covering any previous structures in the apex zone (Fig. 3A).

At the end of the experiment, the sand was carefully removed to observe the silicone topography (Fig. 3C). It shows the well-developed thrust rooted within the silicone in both arc limbs. In front of the apex, two silicone sheets are also observed.

Thrusts and backthrusts, where silicone is present, developed during the early deformation stage of Model 2. Both normal and strike-slip faults nucleated mostly where the silicone pinches out (*e.g.,* Faults 2 and 5; Fig. 2B.1). As deformation proceeded, new thrusts formed and the fold-and-thrust belt evolved asymmetrically: where floored by silicone, the deformation front propagated farther producing a prominent salient (*e.g.,* Faults 14 and 18; Figs. 2B.2 and 3B). In the vicinity of the along-strike boundaries between sand and silicone (dashed lines in Fig. 2B), a set of strike-slip faults associated with normal ones acted as transfer zones. Due to vertical axis rotations of previously nucleated structures, some thrusts of the most internal part of the fold-and-thrust belt can evolve to transpressive bands (Fig. 2B.3), especially in the left arc limb (Fig. 3B). Finally, some diapirs evolved to silicone sheets developed at the arc tips and in the most frontal part of the wedge.

Cross-sections parallel to the transport direction (Figs 3D and 3E) illustrate the differences on the structural style between bands with or without viscous detachment. When silicone is present, a wide fold-and-thrust belt with pop-up and pop-down structures root within the silicone (Fig. 3D); when silicone was absent, a narrow and thick, foreland verging fold-and-thrust belt developed. This belt was detached at the bottom of the sand pack (Fig. 3E).

Discussion

The resulting fold-and-thrust belts show some similarities (*e.g.,* strain partitioning modes or block rotations) with previous ex-
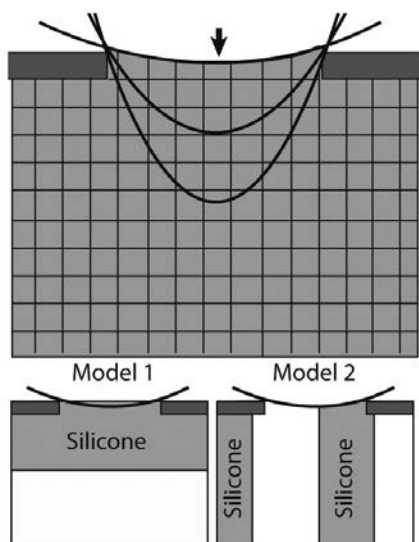

Fig. 1.- Simplified sketch of the experimental apparatus in plan view (black lines show the backstop geometry at different stages of the experiment) and set-up of Models 1 and 2.

Fig. 1.- Esquema simplificado del dispositivo experimental en planta (las líneas negras curvas representan la geometría del backstop en distintos estados) y dispositivo de los Modelos 1 y 2.

Brittle-ductile analogue models of fold-and-thrust belts developed during progressive arching: the effect of viscous basal layer pinch-outs

GEOGACETA, 64, 2018

periments that used the same rig (Jiménez-Bonilla *et al.*, 2016a; Crespo-Blanc *et al.*, 2017; Figs. 2 and 3). However, the presence of silicone pinch-outs generates significant differences. In Model 1, the pinch-out perpendicular to the AMD, constrained the location of the deformation (Figs. 2 and 3A). In Model 2, where pinch-outs are parallel to the AMD,

along-strike differences in structural style are controlled by contrasting basal layer rheology (Figs. 2 and 3B), as observed in previous works (*e.g.,* Cotton and Koyi, 2000).

In the Gibraltar Arc, the distribution of Triassic evaporites greatly controlled the structural style and the evolution of the fold-and-thrust belt (Crespo-Blanc, 2008; Jiménez-Bonilla *et al.*, 2016b). Moreover, some olistostromic units described both onshore and offshore in the Gibraltar Arc (*e.g.,* Medialdea *et al.*, 2004) have been related to parallel pinch-outs in the fold-and-thrust belt. That is the case of the olistostromic units localized in front of an evaporite pinch-out in the Central Betics (Jiménez-Bonilla *et*
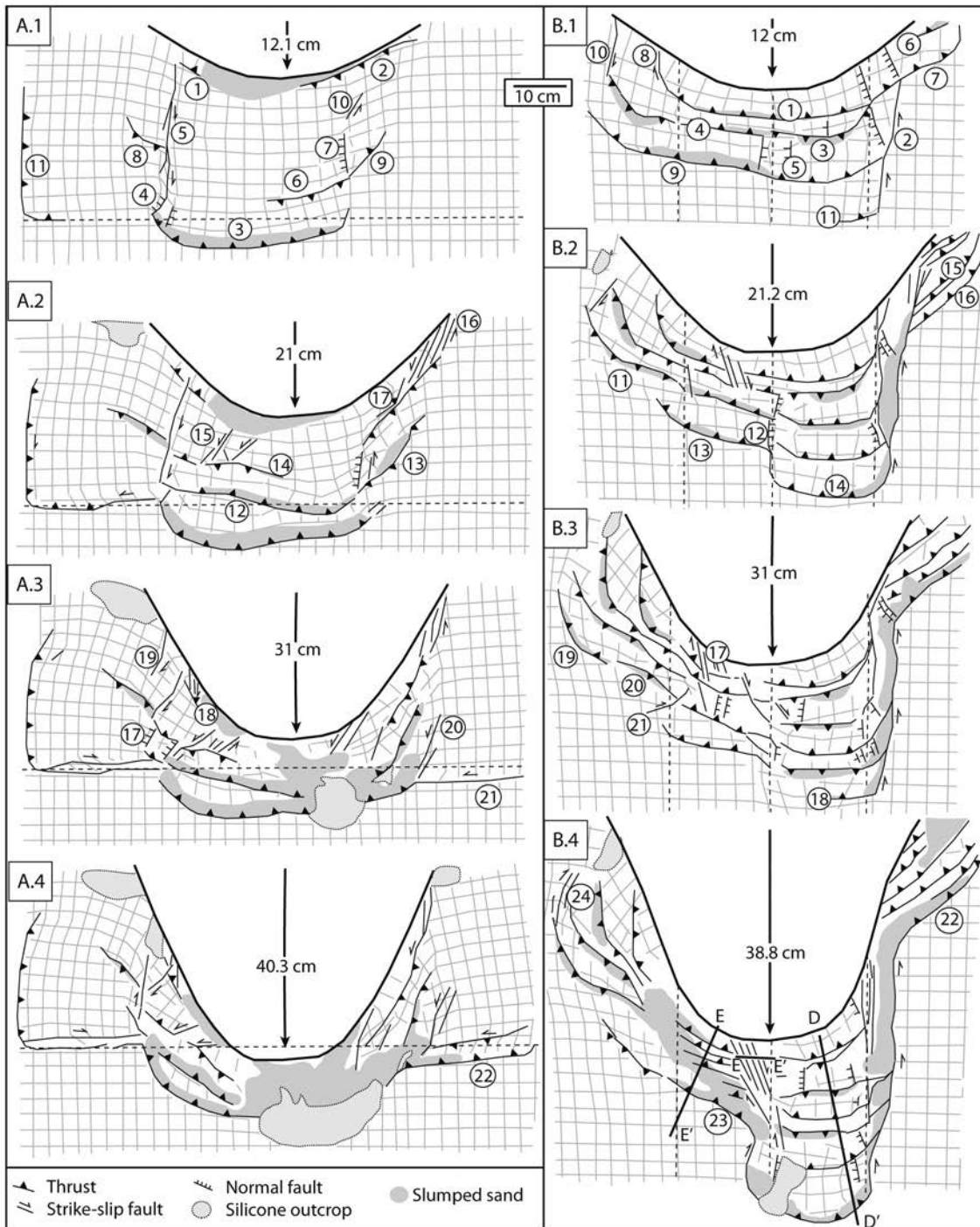

Fig. 2.- A) and B) Line drawings of Models 1 and 2, respectively, showing the progressive deformation in 4 different deformational stages. Dashed lines mark the pinch-outs of the underlying silicone. Numbers: structure chronology. TP: transpressive band

Fig. 2.- A) y B) Dibujos de los Modelos 1 y 2, respectivamente, mostrando la deformación progresiva en 4 estados deformacionales. Las líneas discontinuas marcan los límites de los afloramientos infrayacentes de silicona. Números: cronología de estructuras. TP: banda transpresiva

al., 2016b). This pinch-out initially localizes the deformation front, and when shortening proceeded, the wedge thickened until its gravitational collapse. This tectonic scenario would be comparable to Model 1.

In contrast, Model 2 is useful to explain along-strike variations on the fold-and-thrust belt. For example, it reproduces transpressive bands localized in salient-recess transitions, reported from the external Betics (e.g., Barcos et al., 2015).

Conclusions

1. In Model 1 the deformation front developed close to the silicone pinch-out, trending perpendicular to the AMD. This facilitated the wedge thickening, its subsequent collapse and the deposition of olistostromic units.

2. In Model 2, the presence of silicone pinch-outs parallel to de AMD produced different structural styles along the fold-and-thrust-belt. The differential displacement of the deformation front was accommodated by transfer zones.

3. Both models shed lights about the deposition of olistostromic units and the evolution of the Gibraltar Arc fold-and-thrust belt. Particularly, they explain the differences in the structural style observed along-strike. These experiments can be helpful to get insight about wedges evolution and the origin of mélange-like units, not only in the Gibraltar Arc, but also in other progressive arcs as those around the Mediterranean.

Acknowledgements

References

Barcos, L., Balanyá, J.C., Díaz-Azpiroz, M., Expósito, I. and Jiménez-Bonilla, A. (2015). Tectonophysics 663, 62-77.

Cotton, J.T. and Koyi, H.A. (2000). GSA Bulletin 112, 3: 351-363.

Crespo-Blanc, A. (2008). Journal of Structural Geology 30(1), 65-80.

Crespo-Blanc, A., Jiménez-Bonilla, A., Balanyá, J.C., Expósito, I. and Díaz-Azpiroz, M. (2017). Geogaceta 62, 15-18.

Crespo-Blanc, A., Comas, M. and Balanyá, J.C., (2015). Tectonophysics 683, 308-324.

Jiménez-Bonilla, A., Crespo-Blanc, A., Balanyá, J.C., Expósito, I. and Díaz-Azpiroz, M. (2016a). Geo-Temas 16, CD-Rom.

Jiménez-Bonilla, A., Torvela, T., Balanyá, J.C., Expósito, I. and Díaz-Azpiroz, M. (2016b). Tectonics 35, 3028-3049.

Medialdea, T., Vegas, R., Somoza, L., Vázquez, J.T., Maldonado, A., Díaz-del-Río, V., Maestro, A., Córdoba, D. and Fernández-Puga, M.C. (2004). Marine Geology 209, 173-198.
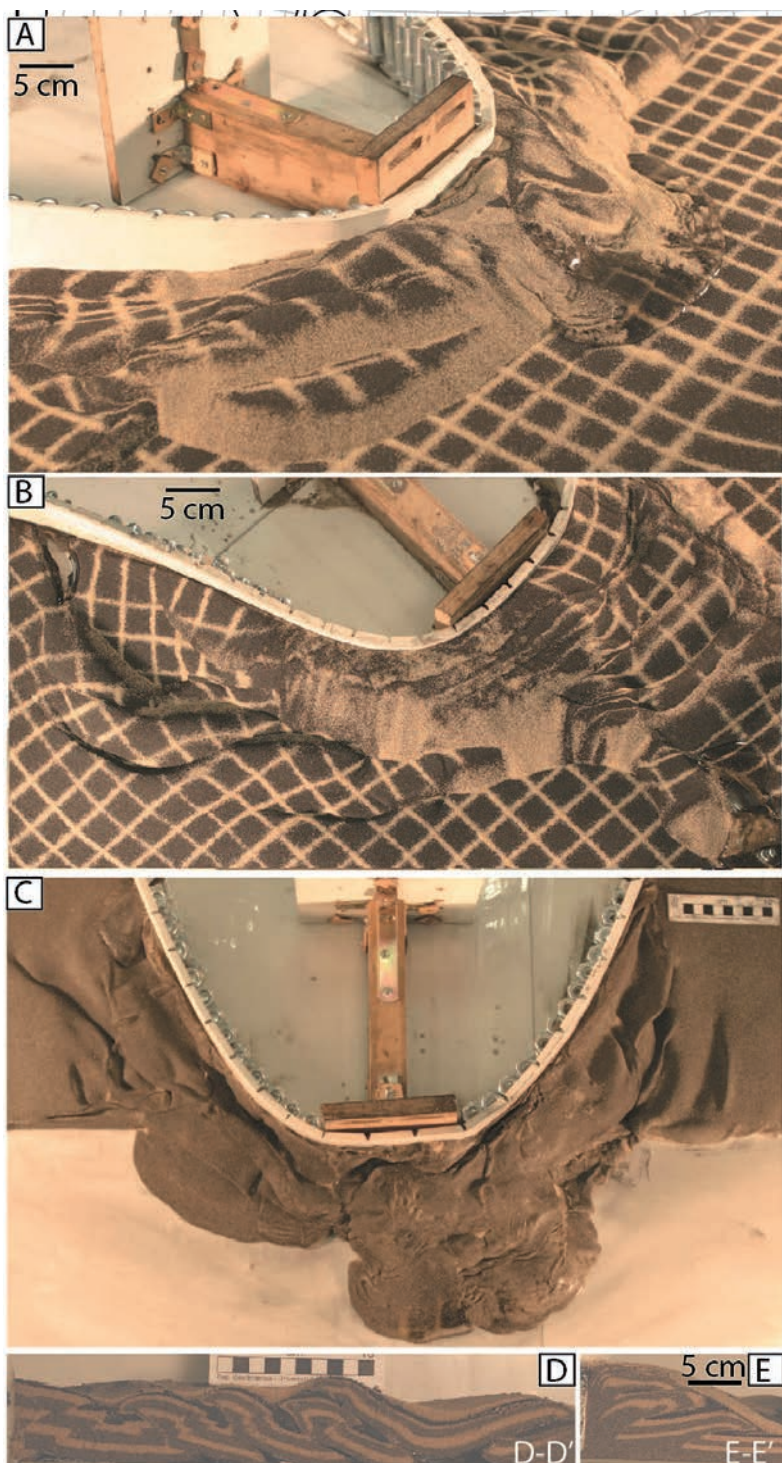

Fig. 3.- Fig. 3.- A) Oblique picture of Model 1. B) Plan view of silicone topography of Model 2 C) and D) Cross-sections in the transport direction of Model 2. See location in Fig. 2B. E) Cross-sections parallel to the transport direction with a silicone and sand detachment levels, respectively. See color figure in the web.

Fig. 3.- Fig. 2.- A) Fotografía oblicua del Modelo 1. B) Fotografía en planta de la topografía de silicona del Modelo 2. C y D) Cortes en la dirección de transporte del Modelo 2. Ver localización en Fig. 2B. y E) Cortes paralelos a la dirección de transporte con un despegue localizado en el nivel de silicona o en la base del prisma de arena, respectivamente. Ver figura en color en la web.